Supporting Information:

Robust production of purified H_2 in a stable, self-regulating, and continuously operating solar fuel generator

Miguel A. Modestino, Karl A. Walczak, Alan Berger, Christopher M. Evans, Sophia Haussener, Carl Koval, John S. Newman, Joel Ager, Rachel A. Segalman.

Electrolyte preparation:

Potassium hydroxide, boric acid and sodium chloride were obtained from Sigma-Aldrich. Solutions of potassium borate were prepared using deionized water, and the pH was determined using an Orion Dual Star benchtop pH meter.

Catalyst deposition:

An AJA Technologies Orion 5 sputtering system was used to deposit the Iridium oxide and Platinum. The Iridium oxide anode was fabricated using reactive sputtering of Iridium with 3 mTorr Oxygen and 3mTorr Argon while holding the substrate at 300°C. The Platinum cathode was deposited at room temperature with a 5 mTorr Argon plasma.

Electrochemical cells fabrication and operation:

The electrochemical cell chassis was fabricated using 3D printing. An Objet 350 Connex printer was used to fabricate the support structures of the cell using a layer-by-layer process. The material of choice for this application was Fullcure RGD720. This material is transparent, ridge plastic and stable in our operating environment. Two electrochemical cells were fabricated for the electrochemical and photoelectrochemical experiments respectively, and are shown in the Figure S1 and S2 below. The cells are composed of two primary chambers separated by a membrane with a small channel joining the chambers. The position, diameter and length of the channel were designed to minimize inadvertent gaseous crossover. The flow between the chambers is actively controlled using a laboratory grade peristaltic pump (Thermo Scientific FH100). The cell used for the electrolysis experiments is substantially larger to allow for collection of small aliquots without disturbing the system. The dimensions chosen for the cells used in the light-driven experiments were selected to match the illumination area from the solar simulator described below (The electrolysis area corresponded to 13.9 cm^2). This cell used amorphous silicon triple junction PV cells from Unisolar and Xunlight, and the high efficiency GaInP2/GaAs/Ge cells were obtained from Spectrolab. A Solar Light XPS150 system was used to simulate AM 1.5 sunlight. The irradiance of the lamp was calibrated using a PMA 2144 pyranometer by Solar Light. Stirring of the each of the cell compartments was used to avoid local concentration gradients at the surface of the electrodes.
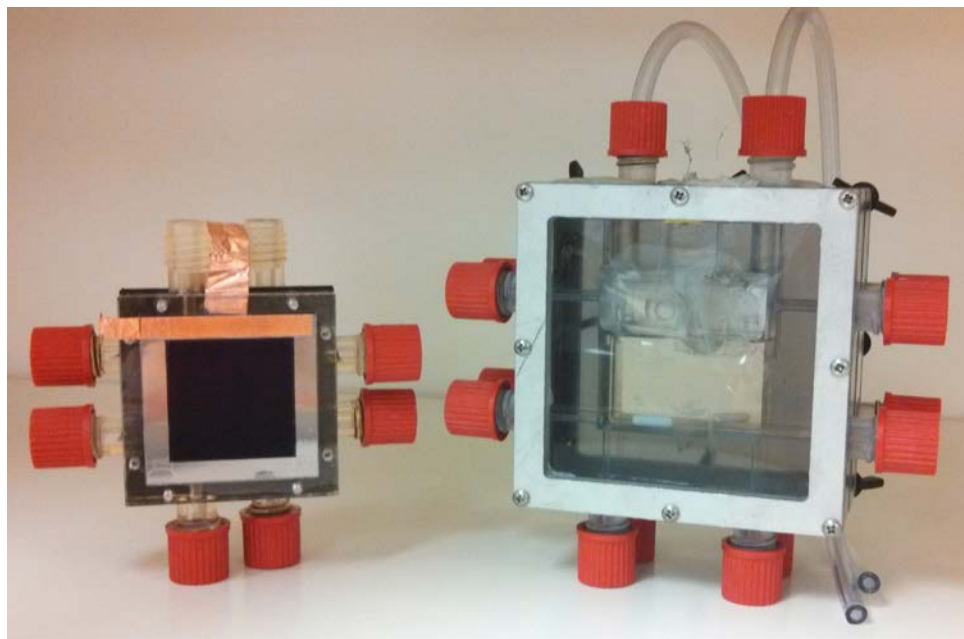
Fig.S1 Images of recirculation prototypes: a) parallel plate solar-hydrogen generator, b) two compartment electrolysis cell. The chassis were custom-built using a 3D printer.
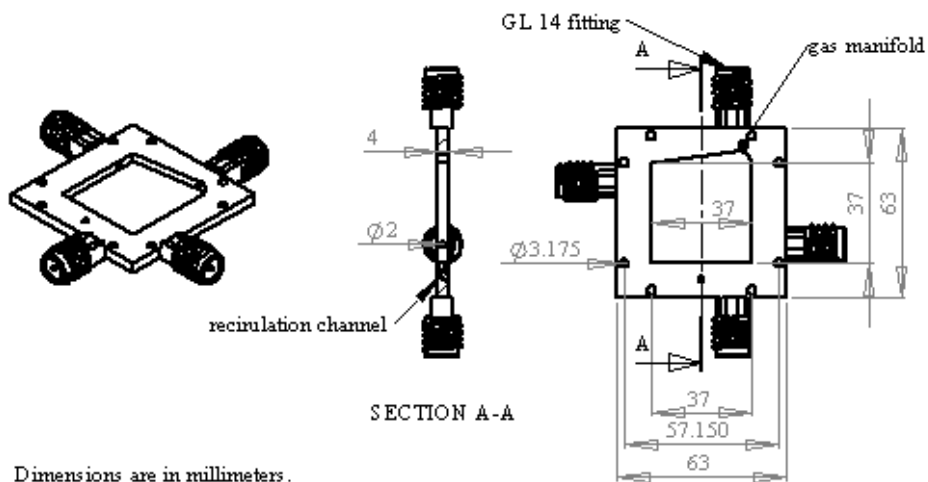

Fig.S2 Schematic of a single side of the parallel plate solar-hydrogen generator.

Electrochemical characterization:

The electrochemical characterization of devices was performed using a VSP-300 potentiostat/galvanostat from Bio-logic. For the chronopotentiometric measurements presented in Fig. 2(A), the current density was fixed at 10 mA/cm^2 based on the membrane area (22.5 cm^2), and the potential was measured between two platinum gauze electrodes (approximately 4 cm^2 in area, 100 mesh woven from 0.0762 cm diameter Pt wire, obtained from Alfa-Aesar). Under these

conditions the initial applied potential to drive 225 mA across the Pt electrodes was equal to 5.25 ± 0.27 V. For the electrocatalytic cell and PV component used in the light-driven water splitting demonstrations, the current densities were measured under no applied bias between electrodes, and the minimum recirculation rate achievable by the peristaltic pump (corresponding to 72 μL/min-cm^2).

Furthermore, the conductivity of Nafion was characterized in 1 M potassium borate solution. A membrane separated H-cell was used, where current was swept across two platinum wires at each side of the cell, and the potential was measured using Ag/AgCl reference electrodes placed in separated compartments that were in contact with the electrolyte via lugging capillaries placed in close proximity to the surface of the membrane.(1) Same measurements were collected with the H-cell connected without a membrane to correct for electrolyte ionic resistance. I-V curves were measured over a period of up to 72 hrs, and showed stable ohmic behavior over time. A typical J-V curve as well as conductivity behavior over time is shown in Fig S3, and the conductivity of the membrane is in the order of 10^{-1} S/cm.
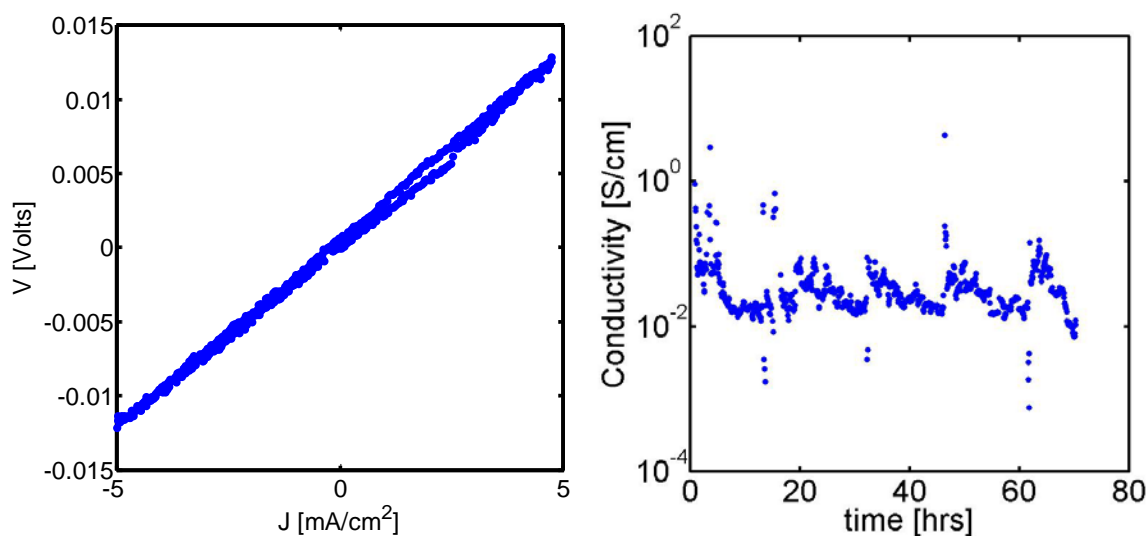

Fig. S3. J-V curve describing potential drop across a membrane equilibrated with 1M potassium borate buffer (left), and conductivity values as a function of time (right).

To characterize the integrated cell used for light driven experiments, we performed AC impedance measurements on the cell separated by a membrane, with an insulator and with an open connection between the oxidation and reduction chambers. The experiments were performed with the recirculation ports connected as well as blocked. Typical results are shown in Fig. S4, and they demonstrate that the resistance of the recirculating cell is 4.2 ohms when a membrane is used for separation and the recirculation port is connected, while the resistance drops to 2.7 ohms when the membrane is removed from the system. It is important to point out that high frequencies (up to 3 MHz) were required to characterize the low resistance cells described in Fig S4(a). In this frequency regime, variations of up to 2 ohms were observed in the impedance measurements from sample to sample, which prevented a detailed characterization of each of the components from the integrated cell. To achieve a better understanding on the conductivity contributions from the recirculation path, the cell was characterized using parafilm to insulate the two chambers and only allow ionic connection through the recirculation channel. Using AC impedance (Fig S4(b)), the resistance with an insulator present was estimated at 1200

ohms, and it is significantly higher than when a membrane is used in the system. Based on these results, for a system operating at 5 mA/cm^2 the fraction of the ionic current passing through the membrane is estimated at more than 99.5%.
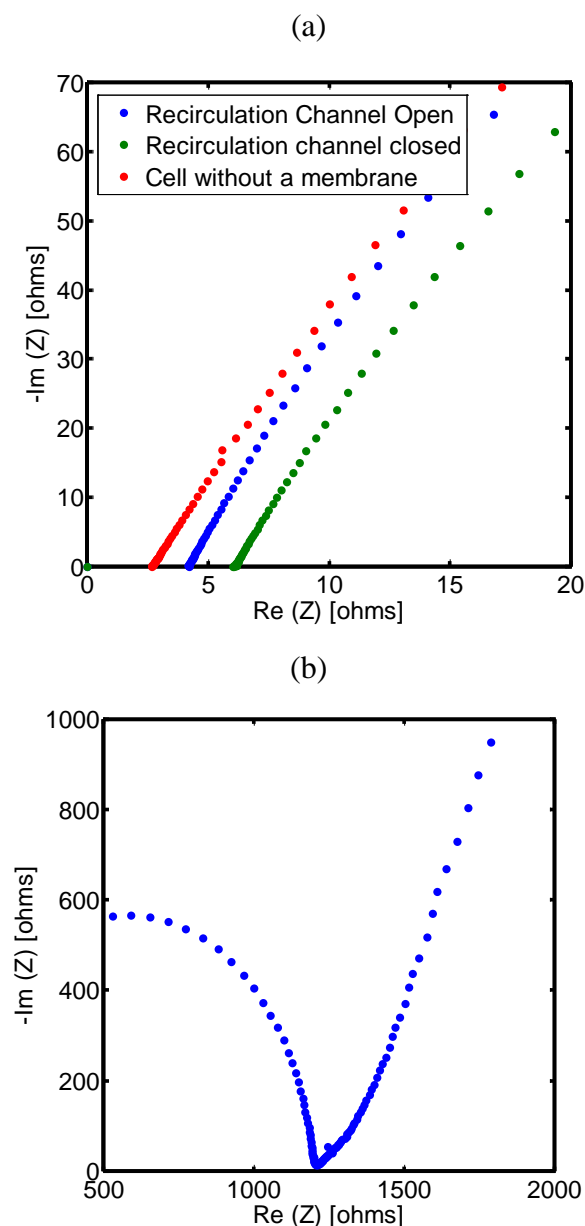
(a)

(b)

Fig S4. AC impedance results from (a) cells with open connections, separated by a membrane and (b) separated by an ionic insulator.

Lastly, to further demonstrate the need of a membrane in the electrochemical cell used in the recirculation experiments, J-V curves were collected for cells separated with a membrane, with an ionic insulator (Parafilm®) and with no separation between reaction chambers. The results presented in Figure S6 demonstrate that (1) operation with an insulator is not possible due to large ionic resistance across the recirculation path that prevent the system to operate at low overpotentials and (2) that the membrane in the system does not provide large amounts of ohmic resistance as the behavior is nearly identical than when it is not present.
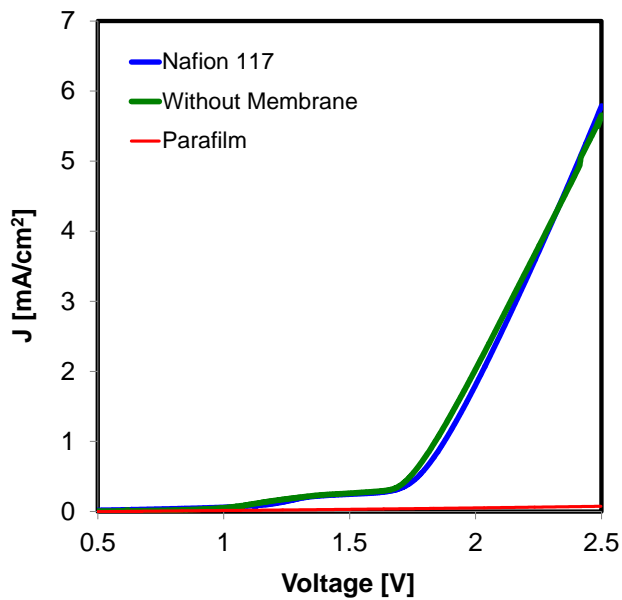
Fig. S5. J-V curves obtained for the electrochemical cell used in solar-driven experiments, using a membrane, parafilm or open space between the two reaction sides.

High efficiency cell results:

The output current from the solar-hydrogen generators fabricated using high efficiency GaInP$_2$/GaAs/Ge cells is presented below. It can be noted that higher current densities are achievable with these cells, both because their better performance (solar cell efficiencies up to 28.3%) and large illumination area (26.6 cm^2). In these devices the ratio of illumination area and area for electrolysis was 1.9.
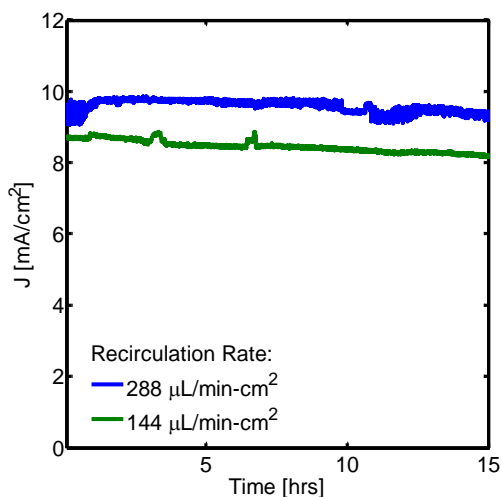

Fig. S6 Current traces obtained from solar-fuel devices fabricated with GaInP$_2$/GaAs/Ge cells. The maximum observed current density in these devices is 9.7 mA/cm^2 and is stable for over 15 hrs of operation.

Gas composition measurements:

Gases were collected in 0.5 L Tedlar® gas sampling bags from streams emanating from each cell compartment. The concentration of O_2 and H_2 gases was determined using a Bruker 430 gas chromatography system, equipped with a 5 Å molecular sieve column and a thermal conductivity detector.

Device efficiency calculations:

The simulation approach follows the modeling work of Delacourt et al. (2) generalized to any number of solution components and reactions, either at the surface or in the bulk.

The scheme is as follows:

n_s = number of species in solution

n_r = number of independent bulk reactions

Governing equations fall into 4 categories:

1. n_s material balances

2. n_s flux equations

3. electroneutrality

4. ns - nr - 1 equations that integrate the total amount of a given species in solution

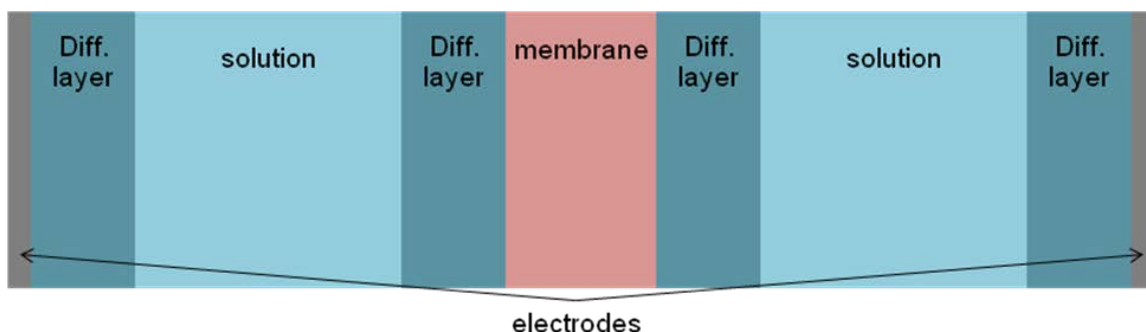The geometry is depicted below:

Fig. S7: Geometry used for 1-D model of electrolysis cell with recirculating streams

In each of the bulk (well-mixed) solutions, the recirculation is added to the model by modifying the material balance equations. For example, in the cathode solution:

$$\nabla \cdot N_i = \sum_l s_{i,l} R_l + \frac{1}{V_{ca}}\left(c_{ib,an} v_{AC} - c_{ib,ca} v_{CA}\right)$$

Here, V_{ca} is the cathode electrolyte volume, $c_{ib,an}$ and $c_{ib,ca}$ are the bulk concentrations of species i in the anode and cathode, respectively, v_{AC} is the volumetric flowrate from anode to cathode, and v_{CA} is the volumetric flowrate from cathode to anode. We can see here why the ratio of the volumetric flow rate to the cell volume is an important parameter in how effectively the recirculation stream limits the buildup of concentration gradients.

After inputting geometric parameters and transport properties into the model, the primary output is the potential between the electrodes as a function of current density and flow rate.

Additionally, the model calculates the composition of the gas streams by performing material balances on hydrogen and oxygen for the system. The following processes are included for both gaseous species:

1. Creation at the correct electrode.

2. Recombination at the opposite electrode.

3. Bulk reaction (unlikely without a homogeneous catalyst but included for completeness).

4. Leaving through the opposite outlet as contaminant.

5. Leaving through the correct outlet as product.

6. Crossing over through either pump stream.

7. Crossing over through the membrane.

Solving the equations gives the flow rate and composition of the two outlet streams. The amount of hydrogen collected will be determined by the partial pressure of hydrogen in the cathode and the cathode outlet flow rate:

$$\dot{n}_{H_2,out} = \frac{P_{H_2,ca}}{RT} v_{out,ca}$$

The collection efficiency is the ratio of this value to the amount of hydrogen generated per unit time at the cathode. The current efficiency is the ratio of the hydrogen produced to the total current density:

$$\eta_I = \frac{P_{H_2,ca} v_{out,ca} n_{H_2} F}{I_{tot} s_{H_2} RT}$$

The total energy efficiency is the product of this current efficiency and the voltage efficiency, which is the ratio of the equilibrium potential, 1.229V, to the total applied potential, which was already mentioned as an output of the model.

$$\eta = \left(\frac{P_{H_2,ca} v_{out,ca} n_{H_2} F}{I_{tot} s_{H_2} RT} \right) \cdot \left(\frac{1.229\ V}{V_{applied}} \right)$$

These three efficiencies (current efficiency, voltage efficiency, and total energy efficiency) are plotted in Figure 1b of the manuscript.

1. Spurgeon JM, Walter MG, Zhou JF, Kohl PA, & Lewis NS (2011) Electrical conductivity, ionic conductivity, optical absorption, and gas separation properties of ionically conductive polymer membranes embedded with Si microwire arrays. *Energy & Environmental Science* 4(5):1772-1780.

2. Delacourt C, Ridgway PL, Kerr JB, & Newman J (2008) Design of an Electrochemical Cell Making Syngas ($CO + H_2$) from CO_2 and H_2O Reduction at Room Temperature. *Journal of The Electrochemical Society* 155(1):B42-B49.